Journal of Power and Energy Engineering, 2021, 9, 1-24
https://www.scirp.org/journal/jpee
ISSN Online: 2327-5901
ISSN Print: 2327-588X

Optimum Sizing and Siting of an Embedded Solar Photovoltaic Generation: A Case Study of 33 kv Sub-Transmission Network at Tarkwa, Ghana

Armstrong Okai Ababio[1], Gabriel Takyi[2], Emmanuel Kwaku Anto[3]

[1]Energy Consulting and Telco Business Directorate, Electricity Company of Ghana Ltd., Accra, Ghana
[2]Department of Mechanical Engineering, Kwame Nkrumah University of Science and Technology, Kumasi, Ghana
[3]Department of Electrical & Electronic Engineering, Kwame Nkrumah University of Science and Technology, Kumasi, Ghana
Email: armstrongokai@gmail.com, gabrieltakyi@yahoo.co.uk, kwakuantoh@yahoo.com

How to cite this paper: Ababio, A.O., Takyi, G. and Anto, E.K. (2021) Optimum Sizing and Siting of an Embedded Solar Photovoltaic Generation: A Case Study of 33 kv Sub-Transmission Network at Tarkwa, Ghana. *Journal of Power and Energy Engineering*, **9**, 1-24.
https://doi.org/10.4236/jpee.2021.93001

Received: February 12, 2021
Accepted: March 27, 2021
Published: March 30, 2021

Abstract

The interconnection of Solar PV to the Tarkwa Bulk Supply Point (BSP) has become necessary in order to provide additional capacity to meet the ever-increasing demand of Tarkwa and its environs during the day. The Solar PV Plant will support the Tarkwa BSP during the day. In this study, a grid impact analysis for the integration of Solar PV plant at three points of common coupling (PCC) at Tarkwa Bulk Supply Point's (BSP) 33 kV network of the Electricity Company of Ghana was carried out. The three PCCs were Tarkwa BSP, Ghana Australia Gold (GAG) Substation and Darmang Substation. Simulations and detailed analysis were carried out with the use of CYME Software (Cyme 8.0 Rev 05). The Solar PV was integrated at varying penetration levels of 9 MWp, 11 MWp, 14 MWp, 16 MWp, 18 MWp, 20 MWp and 23 MWp (representing penetration levels of 40%, 50%, 60%, 70%, 80%, 90% and 100%, respectively) of the 2020 projected light demand of Tarkwa BSP 25.15 MVA network at an average power factor of 0.903. From the study, the optimum capacity of Solar PV power that could be connected is 9 MWp at an optimum inverter power factor of 0.94 lagging, and the GAG Substation was identified as the optimal location. The stiffness ratio at the optimal location was determined as 41.9, a figure which is far greater than the minimum standard value of 5, and gives an indication of very little voltage control problems in the operation of the proposed Solar PV interconnection. The integration of the optimum 9 MW Solar PV Plant to the Tarkwa network represents an additional 12.77% capacity, decreased the technical losses by 7.76%, and increased the voltage profile by 1.97%.

Keywords

Grid Integration, Embedded Solar PV, Sub-Transmission Network, Technical Losses

1. Introduction

Global warming (GW) is a challenge to our world's delicate ecosystems, and could quickly relegate many animal species to extinction. To stop the GW catastrophe, the imminent global warming should be held below 1.5˚C above pre-industrial temperatures. To make this target a reality, global greenhouse gas emissions from fossil fuel burning should be reduced, and the emissions from their 1990 levels reduced by 80 percent worldwide by 2050 [1]. The growing demand for electricity, however, complicates this task. Electricity currently accounts for 12% of total global energy consumption; and, this percentage is projected to rise in the future to 34% of total energy consumption by 2025 [2]. The use of renewable energy sources, such as wind and solar to produce electricity offers alternative solutions to the traditional fossil fuel-based generations, as these renewables are safe, emission-free and environmentally friendly. However, as the level of photovoltaic electricity penetration begins to increase, utilities begin to face new non-traditional problems, one of which is the intermittent nature of solar energy [3] [4]. The power system has to tackle not only uncontrollable demand but also uncontrollable generation [2].

The application of PV systems in power systems as a safe and clean source of energy from the sun can be divided into two main fields including stand-alone and grid-connected applications. Stand-alone PV systems are able to provide power for remote loads that do not have any access to power grids, whereas grid-connected applications can be used to provide energy for local loads as well as to the exchange power with utility grids. PV systems are able to improve the performance of the electric network by reducing the energy losses of distribution feeders, maintenance costs and loading of transformer tap changers during peak hours. Nonetheless, in comparison with other renewable energy-based power resources, PV systems may cause some adverse effects to the system such as harmonic pollution, high investment cost, low efficiency and reliability which hinder their widespread use. Moreover, variations in solar irradiation can cause power fluctuations and voltage flickers and subsequently undesirable effects of high penetrated PV systems on the electric network. In addition, any unintentional islanding in the presence of PV systems may increase the risk of damage to personnel and the other parts of the system components, which can decrease the reliability of the system. Therefore, accurately analyzing the impacts of installing such technology on the performance of the electric network is quite necessary to provide feasible solutions for potential operational problems that grid-connected PV systems can present for distribution systems and their components. In recent decades, the presence of photovoltaic (PV) systems is increased to provide power for local or remote loads. However, when a large PV system connects to the distribution network under variable weather conditions, it may cause severe problems for power system components [5].

In this study, the impact of solar photovoltaic power on sub-transmission network is analyzed with the view to determining the solar plant's optimal penetration level, the optimal position in the network, as well as the optimal inverter's power factor. This information will be of interest particularly to the ECG, and generally to other Power Utility Companies and Researchers. The Tarkwa BSP network is used as the case study system.

2. PV Integration Issues

Electricity demand is not constant. It varies across the year, and even every day. The underlying consumption patterns of residential, commercial and industrial customers drive variations in intra-day demand. The varied combination of customers and demand profiles results in one or more significant system peaks over each 24-hour cycle for almost all systems. For the optimization study, analysis of load profile of the network under study is critical. The solar PV plant must generate adequate electric power to meet the load demand and prevent reverse power flow into the sub-transmission system.

The integration of PVs into a distribution network, if optimally sized and sited, will result in the reduction of technical losses, improvement in voltage profile at various locations in the network, additional capacity of power, among others. Integrating PVs into the distribution network, however, will lead to higher network fault rates which will necessitate the upgrade of switchgear specifications. Additionally, there are concerns regarding power quality violations with respect to the voltage, power factor and other technical shortcomings of the distribution network if the PVs are not adequately designed and situated [6]. The high incorporation of PVs can also contribute to reverse power flow. This bidirectional flow of power will affect the efficiency of existing safety relay schemes.

Some key technical challenges that could be encountered as a result of solar PV injection into the distribution grid are briefly discussed in the following subsections:

2.1. Impacts on Distribution Systems of Large-Scale Solar Photovoltaic Integration

By increasing the penetration level of photovoltaic systems, the distribution networks and their components are more likely to face operational problems. The extent of problems that arise depends directly upon the size (penetration level) of PV and location (siting) of the installation [5].

2.1.1. Inrush Current

The difference between the PV system voltage and the grid voltages may introduce an inrush current that flows at the connection time between the PV system and the utility grid, decaying at an exponential rate to zero. The inrush current so generated can cause disturbance, thermal over stress and other problems [7].

2.1.2. Unexpected Islanding and Safety of Personnel

One of the key issues regarding PV systems integration is the safety issue due to the unexpected islanding on the grid side at the time of fault occurrence. In this case, the photovoltaic systems tend to power the load even after the network is disconnected from the utility grid, and this can give employees electrical shock [8].

2.1.3. Overvoltage in Distribution Network

PV systems are most frequently configured to run close to unity power factor to allow maximum use of solar power. In this situation, the PV system injects only active power into the utility grid which may alter the system's reactive power flow. The voltages of nearby buses can therefore be increased due to reduced flow of reactive power [9]. This overvoltage can have negative impacts on the reliable operation of both utility and customer sides.

2.1.4. Fluctuation/Intermittent Nature of PV Power Output

The fluctuation of the power output of PV systems is recognized as one of the key factors that could cause severe operational problems for the utility network. The power fluctuation phenomenon is due to changes in solar irradiance induced by cloud movement and can continue for a few minutes to hours, depending on the wind speed, the shape and size of the moving clouds, the area covered by the PV system and its topology. Power fluctuations can cause power swings in lines and cables, over- and under-loadings, excessive voltage fluctuations and voltage flickers [10].

2.1.5. Harmonics

Harmonic distortion is a serious problem of power quality, which may occur in PV systems due to the use of power inverters to convert DC current to AC. The produced harmonics can cause parallel and serial resonances, overheating in capacitor banks and transformers as well as incorrect or nuisance operation of protection systems which can reduce the reliability of power systems [11].

2.2. Solar Energy and Duck Curve

In utility-scale electricity generation, the so-called duck curve shows the timing disparity between peak demand and renewable energy production over a day. In many energy markets, the highest demand occurs after sunset, when solar power is no longer available. For areas where a large amount of solar energy has been installed, the amount of power to be produced from sources other than solar or wind shows a rapid increase around sunset and peaks in the mid-night hours, creating a graph that resembles the outline of a duck. At any given time of the day, the duck curve indicates the demand for electricity [12]. Electricity firms produce the least amount of electricity overnight, then it ramps up in the morning (due to increase in demand), then at sunset, energy demand peaks as shown in Figure 1.

Figure 2 shows the solar production and variation of demand curve over the day. The change in demand curve is shown with the increase in solar deployment over years. Maximum solar panel deployment is taking place and it is found that the sun produces most of the energy at the mid-day. New solar plants are being constructed yearly which makes mid-day demand drop substantially. This drop in the mid-day demand explains the formation of the "Belly of the Duck Curve" [12].

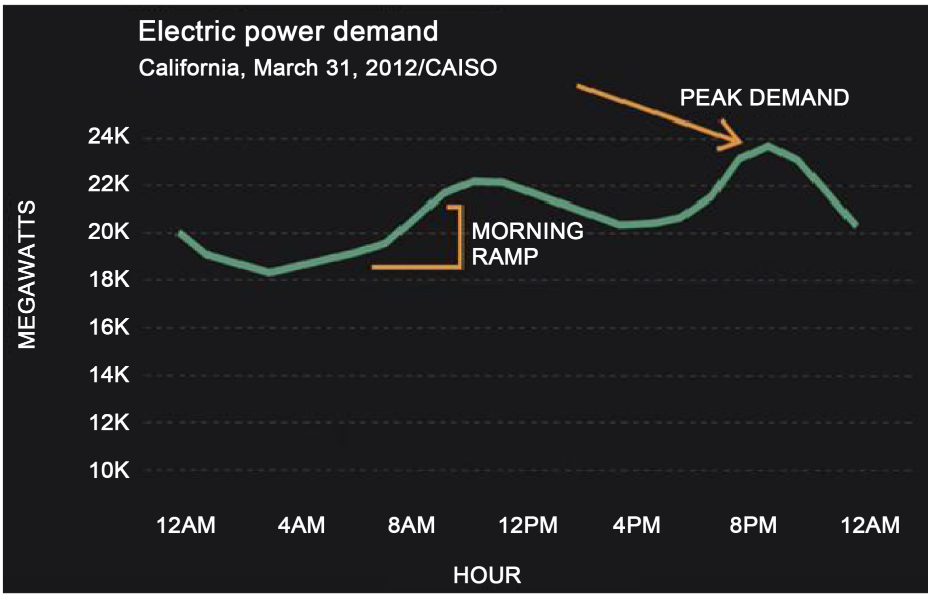

Figure 1. Electric power demand for 24 hours [12].

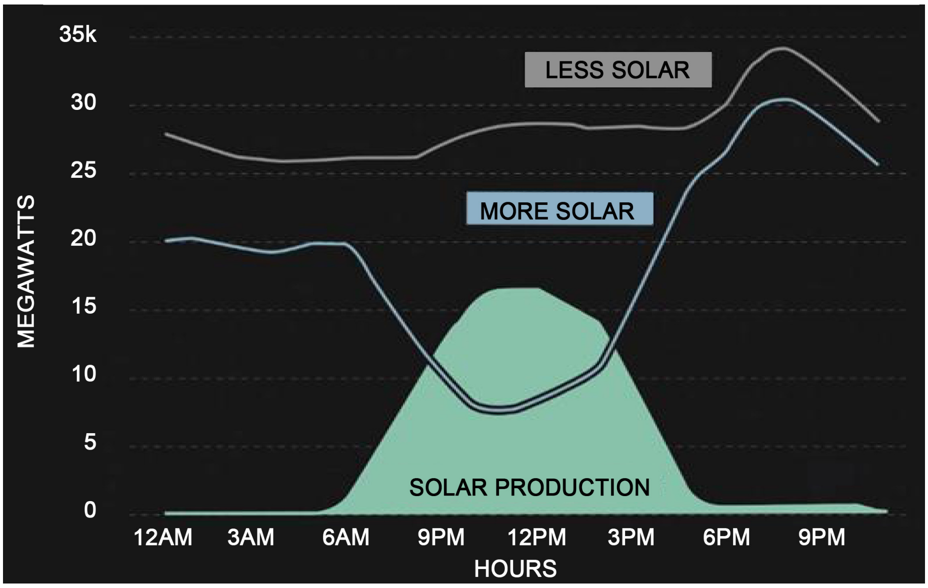

Figure 2. Decrease in demand due to increase in solar production [12].

2.3. Stiffness Ratio

The stiffness ratio is determined at the Point of Common Coupling (PCC) for the solar PV Integration. The PCC is where Solar Plant is connected to the Distribution network. Stiffness Ratio (SR) is the ratio of the anticipated short circuit capability (in MVA) at the PCC to the PV plant output [13]. It is given as:

$$\text{Stiffness ratio} = \text{SC}_{\text{PCC}} / \text{PV}_{\text{output}}$$

where SC_{PCC} is the maximum Short Circuit level at the Point of Common Coupling and the $\text{PV}_{\text{output}}$ is the power output or rating of the solar PV.

Stiffness ratio *gives a measure of the ability of a Distribution network to prevent voltage violations or deviations caused by Solar PV integration into the Grid*. As best practice in the industry, S.R > 5 is considered to be adequate [13].

2.4. Inverter Power Factor

At one point, if the PV array (as after sunset) produces no real power, an inverter will supply only reactive power Q (kVAR). On the other hand, when the PV array generates its maximum rated real power, the inverter has no ability to produce reactive power unless it is deliberately over dimensioned or a part of active power output is truncated. Under such constraints, the PV inverter's reactive power can be regulated by its power factor in such a way that the Solar PV inverter does not exceed its kVA rating. However, reactive generation of power by a PV inverter is not free, and comes at a cost [14]. The power factor of the inverter is therefore a key factor in determining the quantum of real and reactive power to be produced by the solar PV plant.

2.5. Solar Irradiation Data

The viability of any solar PV installation at any location depends, to a large extent, on the availability of solar radiation at that location. To determine the availability of solar radiation at any location, the global horizontal irradiance (GHI) is measured. The GHI refers to the power per unit area received from the Sun in the form of short wavelength electromagnetic radiation measured perpendicular to the incoming sunlight. GHI is expressed in W/m^2 and comprises of direct normal irradiance and diffuse horizontal irradiance. Direct normal irradiance refers to the part of the GHI that falls in a straight line at its present location in the atmosphere from the direction of the sun. Diffuse horizontal irradiance refers to the GHI portion that does not come from the sun on a direct path, but has been dispersed through clouds, particles of dust, vapor molecules etc. Various national and international bodies collate the GHI for various locations throughout the world all year round. The collated GHI is used to plot solar maps for the various locations and countries (see **Figure 3**).

The solar maps provide information on grid cells on a month or annual average daily total of solar resources.

Figure 4 shows the climatic and solar irradiation data for Prestea, a town in the environs of Tarkwa. From **Figure 4**, it is evident that the seasonal variation

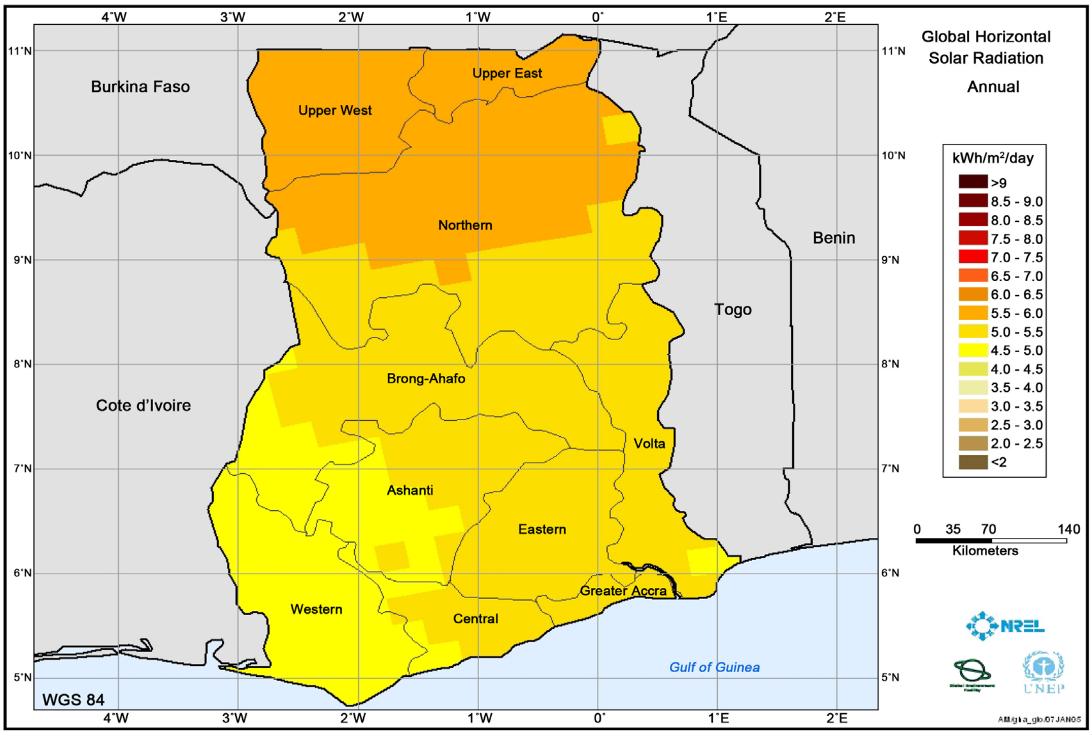

Figure 3. Annual daily average global horizontal irradiance plot for Ghana [UN Environment Program (UNEP), National Renewable Energy Laboratory (NREL)].

Month	Air temperature	Relative humidity	Precipitation	Daily solar radiation - horizontal	Atmospheric pressure	Wind speed	Earth temperature	Heating degree-days 18 °C	Cooling degree-days 10 °C
	°C	%	mm	kWh/m²/d	kPa	m/s	°C	°C-d	°C-d
January	25.3	77.5%	34.62	5.11	99.9	2.8	26.1	0	473
February	25.5	81.4%	54.19	5.23	99.9	2.9	26.4	0	433
March	25.8	83.7%	123.22	5.23	99.8	2.8	26.8	0	489
April	26.0	84.1%	175.04	5.15	99.8	2.6	27.0	0	479
May	25.7	85.5%	211.67	4.80	100.0	2.3	26.6	0	487
June	24.7	86.0%	229.61	4.02	100.2	2.4	25.3	0	442
July	23.8	84.8%	109.73	4.05	100.3	2.9	24.4	0	428
August	23.7	83.6%	39.87	3.92	100.3	2.8	24.3	0	424
September	24.2	84.8%	122.83	3.87	100.1	2.6	24.8	0	425
October	24.7	85.6%	196.63	4.54	100.0	2.5	25.3	0	455
November	25.1	84.2%	111.33	4.88	99.9	2.2	25.8	0	454
December	25.2	81.6%	62.25	4.88	99.9	2.6	25.7	0	470
Annual	**25.0**	**83.6%**	**1,471.00**	**4.64**	**100.0**	**2.6**	**25.7**	**0**	**5,457**
Source	NASA	NASA	NASA	NASA	NASA	NASA	NASA	NASA	NASA
Measured at					m	10	0		

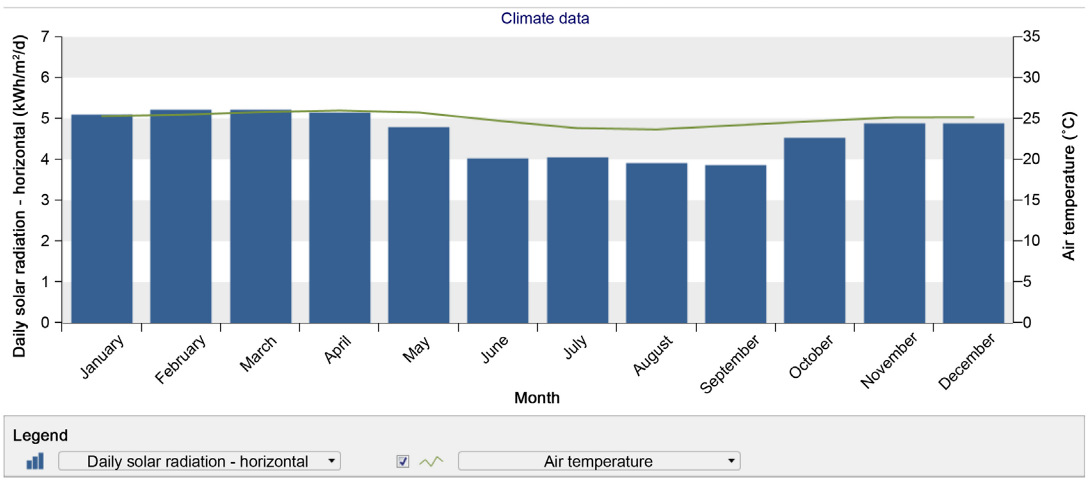

Figure 4. Prestea-Tarkwa solar irradiation data (Source: RETScreen International).

in the country impacts the GHI measured in the Prestea-Tarkwa area. From November to May, the GHI is above the annual average of 4.64 kWh/m^2/d with the peak GHI of 5.23 kWh/m^2/d recorded in February and March. During the rainy season, the GHI recorded for the area is below the annual average with the lowest GHI of 3.87 kWh/m^2/d recorded in September. The recordings are within acceptable limits.

2.6. Typical Daily Solar PV Plant Output Profile

In Ghana, due to the equatorial location and tropical climate, a typical solar PV plant's generation occurs during daytime hours starting from around 6:00 GMT. The power generated by the PV plant increases gradually until it peaks during the noon hours and gradually reduces to zero in the evening around 18:00. **Figure 5** shows the generation profile of an existing Solar PV plant in ECG's network. This study considers the load profile of the selected network from 7:00 to 17:00 in order to select the optimum size of the PV plant [6].

3. Case Study System—Tarkwa BSP Network

This research focuses on Grid Impact Study for the integration of Solar PV Plant into the Tarkwa BSP. Tarkwa is the capital of Tarkwa-Nsuaem Municipality in the Western Region, southwest of Southern Ghana. Tarkwa, as at 2017, had a settlement population of 175,868 people which comprises 49.2% females and 50.8% male [15]. Tarkwa is noted for gold and manganese mining.

Figure 6 shows the geographic layout (Google Map) of Tarkwa. It boasts of a University of Mines and Technology (UMaT). Tarkwa and its environs is served by the Tarkwa Bulk Supply Point (BSP) of the Electricity Company of Ghana Ltd (ECG). The Tarkwa BSP has three 25/33 MVA 161/34.5 kV power transformers. The 34.5 kV side of this power transformers is connected to the ECG 33 kV single bus bar which sectionalizes through 500 mm^2 copper cross-linked polyethylene (XLPE) cables. Emanating from the 33 kV busbar are seven outgoing feeders serving Tarkwa Primary Substation (one feeder), Golf Fields Village (one feeder), Abosso (two feeders), Bonsa (one feeder) and Teberebie (two feeders).

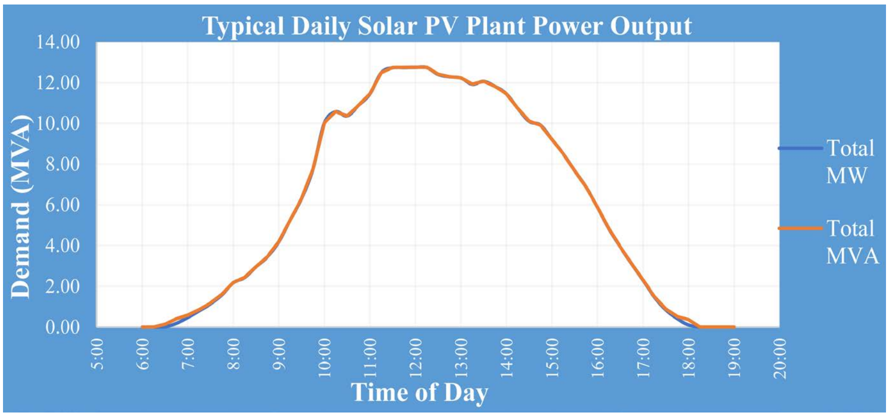

Figure 5. BXC Mankoadze 20 MWp solar PV power generation on 26th January 2017.

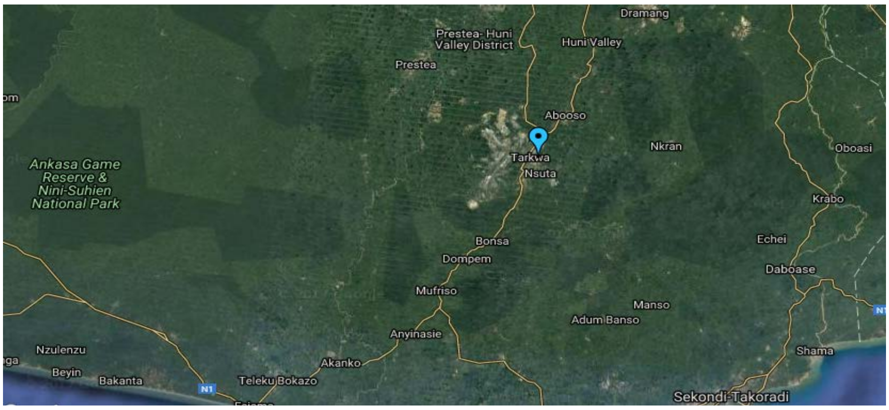

Figure 6. Geographical location of Tarkwa (Source: Google earth).

Each outgoing feeder has secondary substations connected where the high voltage is stepped down to low voltage (400/230 V) for onward distribution to customers.

Figure 7 shows the single line diagram of the Tarkwa BSP network which comprises three outgoing feeders to connect Abosso Primary Substation and Darmang Primary Substation, Tamso Primary Substation and the Ghana Australia Gold (GAG) Primary Substation. The interconnection of Solar PV to the Tarkwa BSP has become necessary in order to provide additional capacity to meet the ever-increasing demand of Tarkwa BSP during the day.

4. Methodology

This section describes the various methodological steps undertaken in the determination of the impact of the PV system interconnection with the main grid. These are:

1) Generation of PV power output profile;
2) Generation of Tarkwa BSP Load Profiles;
3) Modeling of Grid-Tied Photovoltaic Network;
4) Load Flow Simulations;
5) Fault Level Simulations;
6) Analyses of the results.

4.1. Generation of PV Power Output Profile

For the optimization study, analysis of the load profile of the network under study is critical. The solar PV plant must generate adequate electric power to meet the load demand and prevent power flow into the sub-transmission system.

In Ghana, owing to its equatorial location and tropical climate, a typical solar PV plant's generation occurs during daytime hours starting from around 6:00. The power generated by the PV plant increases gradually until it peaks during the noon hours and gradually reduces to zero in the evening around 18:00 (see **Figure 5**). Thus, this study considers the load profile of the selected network from 7:00 to 17:00 in order to select the optimum size of the PV plant.

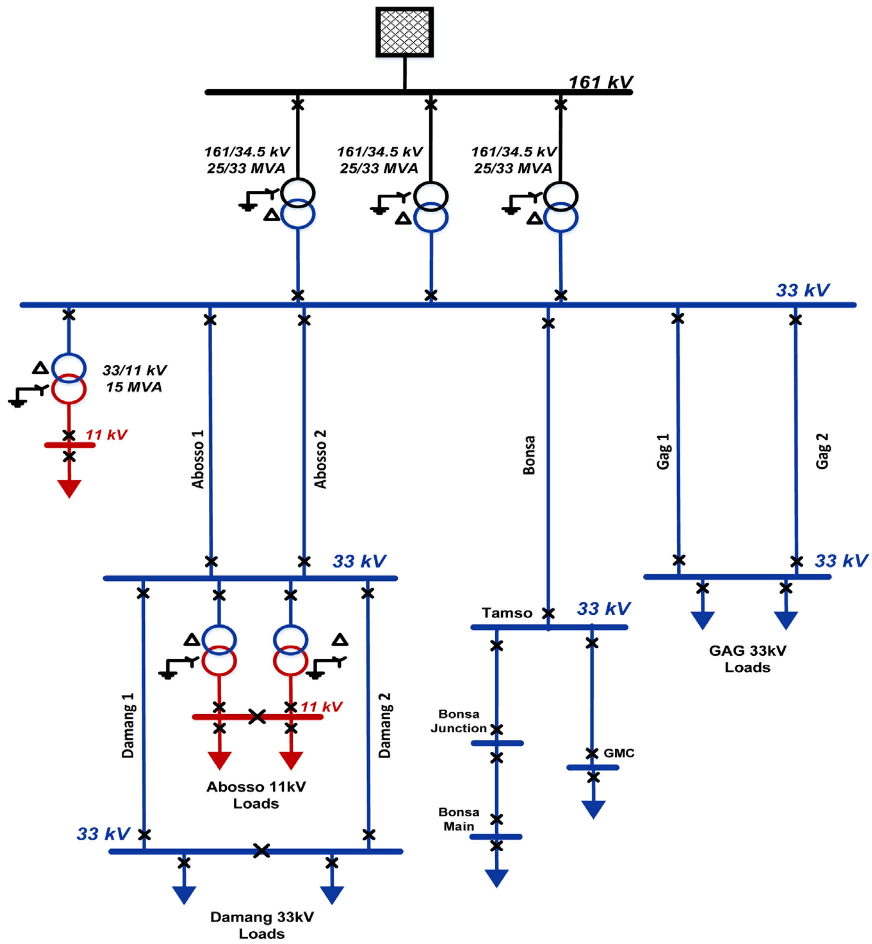

Figure 7. Single line diagram of the Tarkwa BSP Network.

4.2. Generation of Tarkwa BSP Load Profile

The load profile of Tarkwa BSP for the year 2019 indicates a peak demand of 41.82 MVA with a corresponding power factor of 0.915 in the month of March. As a result, the average weekday and weekend daily demand was calculated from the 24-hour demand profile obtained from the ECG Automatic Meter Reading (AMR) online system for the month of March to enable us determine the penetration level of Solar PV plant to be connected to the Tarkwa BSP. Table 1 and Figure 8 show the average ***weekday*** demand profile for Tarkwa BSP, whereas Table 2 and Figure 9. show the average ***weekend*** demand profile for Tarkwa BSP for the month of March, 2019.

From Table 1 and Figure 8, the weekday peak demand of the average load readings in March was recorded as 31.34 MVA with a corresponding power factor of 0.921 at 21:00. From Table 2 and Figure 9, the weekend peak demand of the average load readings in March was recorded as 29.89 MVA with a corresponding power factor of 0.928 at 23:00.

The minimum demands recorded for weekday and weekend were 20.45 MVA with a power factor of 0.913 and 24.29 MVA with power factor of 0.912, respectively. The weekday demand profile was higher than the weekend demand

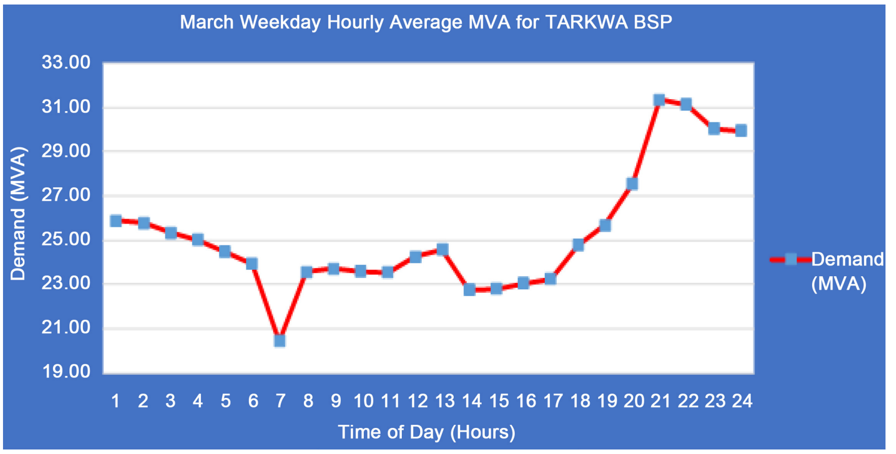

Figure 8. Weekday hourly average load profile for Tarkwa BSP for March, 2019.

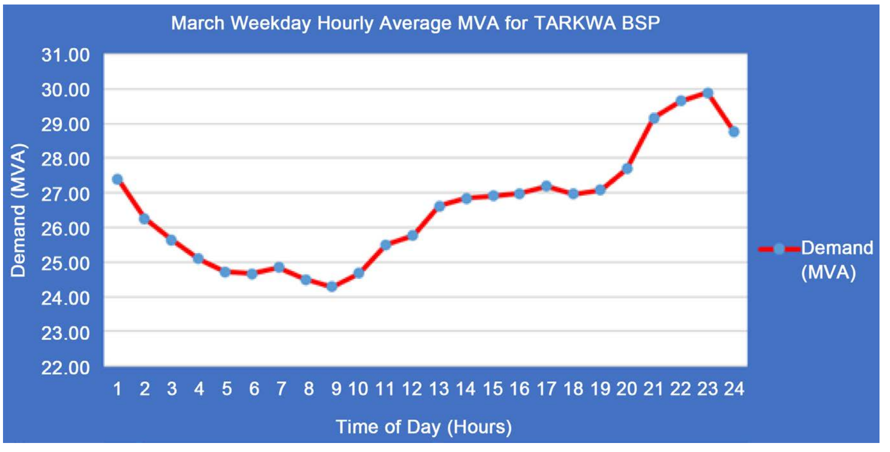

Figure 9. Weekends hourly average load for Tarkwa BSP for March, 2019.

profile as can be seen from Figure 8 and Figure 9 respectively. Using an annual growth rate of 3.62%[1], the average weekday demand profile was projected to 2020. The weekday 2020 projected demand for Tarkwa BSP is shown in Figure 10.

The Tarkwa BSP serving the Tarkwa network recorded an average weekday and weekend load factors of 0.806 and 0.888 respectively. This shows a high utilization of power. The network is made up of a mix of industrial and residential customers. There is one significant peak which occurs in the evening and relatively flat demand profile during the daytime.

4.3. Modelling of Grid-Tied Photovoltaic Networks

In this study, the existing Tarkwa BSP operational network was modelled using the CYME Power Engineering Software (Cyme 8.0 Rev 05). For the modelled network, three points of common coupling (PCCs) for the solar PV plant were considered. The PCCs selected from the Tarkwa BSP network were:

1) Interconnection at the **source bus** (Tarkwa BSP).

[1]ECG system planning 2019 *ENERGY AND DEMAND FORECAST REVIEW*.

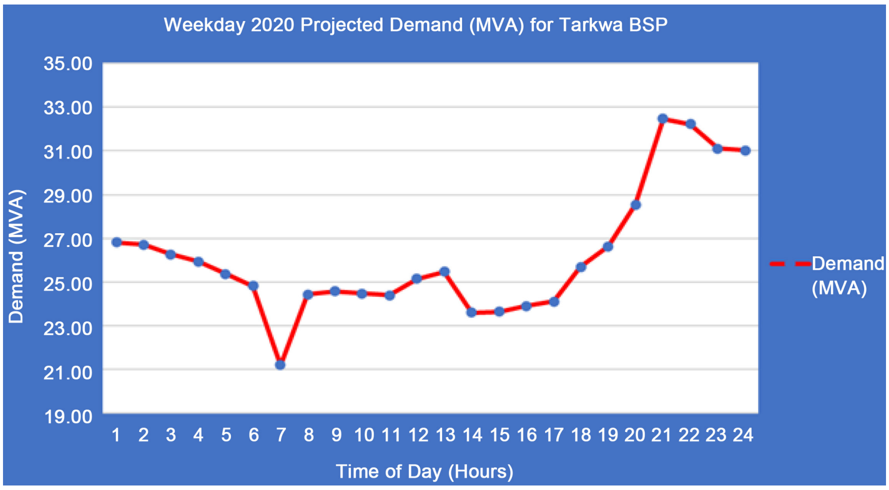

Figure 10. Weekday 2020 projected demand (MVA) for Tarkwa BSP.

Table 1. March weekday average profile.

Time of Day (Hours)	KW	Demand (MVA)	Power Factor
1	23.68	25.88	0.918
2	23.56	25.77	0.918
3	23.12	25.34	0.917
4	22.87	25.03	0.918
5	22.34	24.47	0.917
6	21.84	23.95	0.916
7	18.64	20.45	0.913
8	21.60	23.57	0.920
9	21.46	23.72	0.909
10	21.25	23.61	0.905
11	21.24	23.54	0.907
12	21.91	24.27	0.909
13	22.16	24.58	0.908
14	20.57	22.77	0.908
15	20.51	22.81	0.905
16	20.70	23.06	0.902
17	21.00	23.26	0.907
18	22.40	24.79	0.906
19	23.25	25.69	0.909
20	25.11	27.55	0.914
21	28.77	31.34	0.921
22	28.59	31.11	0.922
23	27.53	30.02	0.921
24	27.38	29.94	0.917

Table 2. March weekend average profile.

Time of Day (Hours)	KW	Demand (MVA)	Power Factor
1	25.24	27.41	0.923
2	24.12	26.26	0.922
3	23.50	25.65	0.920
4	23.04	25.10	0.922
5	22.73	24.72	0.924
6	22.60	24.66	0.920
7	22.73	24.85	0.919
8	22.37	24.50	0.917
9	22.04	24.29	0.912
10	22.37	24.69	0.911
11	23.09	25.50	0.912
12	23.32	25.77	0.910
13	24.09	26.62	0.910
14	24.40	26.85	0.913
15	24.52	26.91	0.915
16	24.67	26.98	0.918
17	24.91	27.19	0.921
18	24.68	26.98	0.920
19	24.71	27.09	0.916
20	25.31	27.70	0.917
21	26.93	29.17	0.927
22	27.40	29.65	0.928
23	27.63	29.89	0.928
24	26.55	28.75	0.927

2) Interconnection at **mid-way** of the network (GAG Primary Substation).

3) Interconnection at the **tail end** of the network (Darmang Switching Station).

Modelling Considerations

The following considerations were made in modelling the networks:

- Average behavior of the load type in the various networks was modeled as constant power loads.
- Based on data obtained from ECG Automatic Meter Reading (AMR) of Tarkwa BSP, the average power factor of the BSP of 0.903 lagging was used for all load points at the Tarkwa BSP.
- An operating voltage of 34 kV was used at the ECG end of the Tarkwa BSP as per ECGs specifications.
- Bus sectionalizers on 33 kV and 11 kV buses of primary substations were considered tied together respectively.

4.4. Load Flow Simulations

The 2018 projected demand for the Tarkwa BSPs was used as the base load for this study. The **12:00 pm** reading of the average weekday profile of March, 2019 obtained from the ECG automatic meter reading (AMR) online system **(24.27 MVA)** was projected to **2020 (25.15 MVA)** and used for the analysis. A corresponding average power factor of **0.903** was used for the load points in the network. The loads were allocated to the load points and substations within the networks.

4.4.1. Assumptions and Planning Considerations Made for the Load Flow Study

- An operating voltage of 34 kV was used at ECG end of the Tarkwa BSP network.
- Constant Power load model was used to represent average behavior of the load type in the network.
- The 33 kV bus voltages were kept between 91% (30.03 kV) and 109% (35.97 kV) *i.e.* ±9%[2]. Bus voltages.
- Outside these ranges were considered **under** and **over** voltages, respectively.

The following loadings limits were also set for network elements as shown in Table 3.

4.4.2. Load Flow Simulation Scenarios

Simulations were carried out to determine the technical losses and voltage impacts after modeling the various existing operational networks. The simulations were done for **three** main scenarios:

1) **Scenario 1**: Determination of optimum solar PV **plant size** at each PCC.

- Load flow simulation with varying penetration levels of 40%, 50%, 60%, 70%, 80%, 90% and 100% of the solar PV plant connected at the three PCCs was carried out. The study considered penetration levels from 40% because the technical impact of the solar PV on the network will be significant from 40% onwards.
- Technical loss and voltage impact analysis in the distribution network was carried out.

2) **Scenario 2**: Determination of optimum solar PV plant **location** and **power factor**.

- Load flow simulation using optimum solar PV plant capacity and location from Scenario 1 and varying power factor of solar PV plant.

Table 3. Limits of loading network elements.

Network Element	Normal Loading (%)	Emergency Loading (%)
Cables	70	100
Overhead lines	70	100

[2]This voltage bandwidth is based on the ECG planning manual.

- Technical loss and voltage impact analysis in the distribution network was carried out.

3) **Scenario 3**: Determination of the **stiffness ratio** at the Point of Common Coupling (PCC) for the solar PV integration.

5. Results and Discussions

The results of network simulations (at the **source**, **midway** and **tail end**) of the various scenarios are presented and discussed here.

5.1. PV Connected at the Tarkwa (Old Atuabo) BSP—Source of the Network

The Solar PV was connected to the source of the 33 kV network of the Tarkwa (Old Atuabo) BSP. The detailed results of the study are presented in Table 4. The voltage profiles at the **Source** (Tarkwa PCC) and technical losses of the network for different Solar PV penetration levels are shown in Figure 11 and Figure 12, respectively.

Discussion of Results—Connection of PV at the Source Tarkwa (Old Atuabo) 33 kV BSP

As the PV penetration level increases at the Tarkwa PCC (Source), the voltage reduces, but nevertheless remains above ECG's allowable voltage lower limit of 30.03 kV, as shown in Figure 11.

The 33 kV feeder losses, on the other hand, progressively increase, as the PV penetration level increases, with the minimum losses occurring at 40% penetration level corresponds to a capacity of 9 MWp as shown in Figure 12.

This implies that 40% PV penetration level optimizes the Tarkwa BSP network

Table 4. Detailed results with Tarkwa bulk supply point as the PCC (Source).

	Interconnected at the BSP							
Network load capacity	22.70	MW	250	Wp				
Total load in kW	22,704.81							
Power Factor of load	0.90							
Penetration level	Before	40.0%	50.0%	60.0%	70.0%	80.0%	90.0%	100.0%
		0.00	**0.00**	**0.00**	**0.00**	**0.00**	**0.00**	**0.00**
Solar PV		0.00	0.00	0.00	0.00	0.00	0.00	0.00
No. of series		16	16	16	16	16	16	16
No. of parallel		5	5	3412	3980	4550	5120	5690
100% output (kW)		0.00	0.00	0.00	0.00	0.00	0.00	0.00
Qty of panels		20,000	20,000	13,648,000	15,920,000	18,200,000	20,480,000	22,760,000
BSP Voltage@unity/kV	33.700	33.670	33.670	33.660	33.660	33.650	33.630	33.620
BSP pf@unity/%	89.66	36.99	2.43	−30.68	−53.77	−67.69	−75.95	−81.01
System losses@unity/kW	167.320	184.040	193.370	204.780	218.300	233.940	251.710	271.650

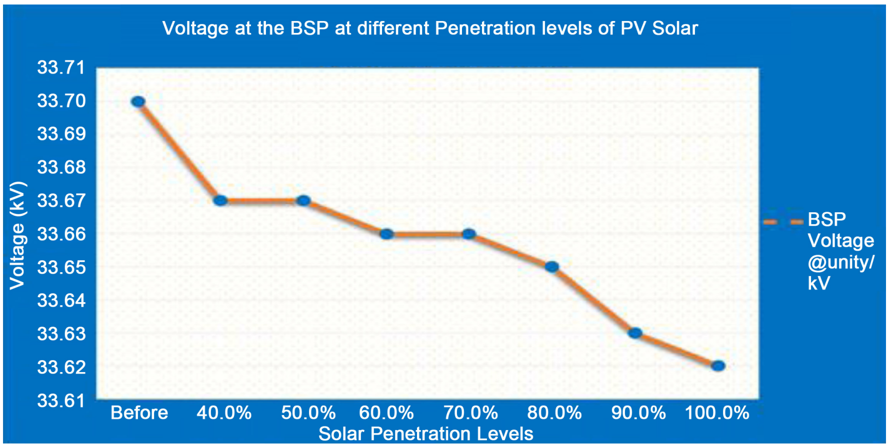

Figure 11. Voltage profile at the source tarkwa (old atuabo) BSP at different solar PV penetration levels.

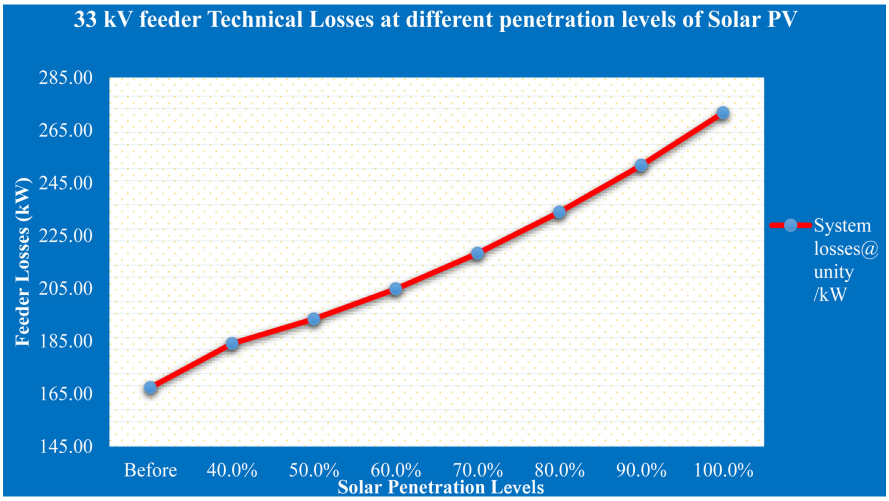

Figure 12. 33 kV feeder technical losses of the Tarkwa (Old Atuabo) BSP network at different penetration levels.

with respect to loss reduction when the Solar PV plant is connected to the Source (Tarkwa BSP).

5.2. PV Connected at the Ghana Australia Gold (GAG) Primary Substation—Midway of the Network

The Solar PV was connected midway of the network at the GAG Primary substation. The detailed results of the study have been presented in Table 5. The voltage profiles at the GAG PCC (midway) and technical losses for different Solar PV penetration levels are shown in Figure 13 and Figure 14, respectively.

Discussion of Results—Connection of Solar PV Plant at the Ghana Australia Gold (GAG) Primary Substation—Midway

As PV penetration level increases at the GAG PCC (midway of the network), voltage profile is improved, but nevertheless remains below ECG's allowable voltage upper limit of 35.97 kV, as shown in Figure 13.

Table 5. Detailed results with Ghana Australia Gold (GAG) primary substation as the PCC (Midway).

				Interconnected at GAG-Bus				
Network load capacity	22.70	MW	250	Wp				
Total load in kW	22,704.81							
Power Factor of load	0.98							
Penetration level	Before	40.0%	50.0%	60.0%	70.0%	80.0%	90.0%	100.0%
		9.08	**11.35**	**13.62**	**15.89**	**18.16**	**20.43**	**22.70**
Solar PV		9.08	11.35	13.62	15.89	18.16	20.43	22.70
No. of series		16	16	16	16	16	16	16
No. of parallel		2275	2843	3412	3980	4550	5120	5690
100% output (kW)		9081.93	11,352.41	13,622.89	15,893.37	18,163.85	20,434.33	22,704.81
Qty of panels		9,101,926	11,372,407	13,648,000	15,920,000	18,200,000	20,480,000	22,760,000
BSP Voltage@unity/kV	33.67	33.67	33.67	33.66	33.65	33.64	33.63	33.61
PCC Voltage@unity/kV	33.38	33.56	33.58	33.61	33.63	33.64	33.65	33.65
BSP pf@unity/%	89.64	62.20	44.35	20.66	−5.24	−28.13	−45.42	−57.41
PCC pf@unity/%	90.18	−99.92	−99.87	−99.81	−99.74	−99.66	−99.57	−99.48
System losses@unity/kW	167.300	154.310	170.550	194.520	226.250	265.760	312.590	367.730

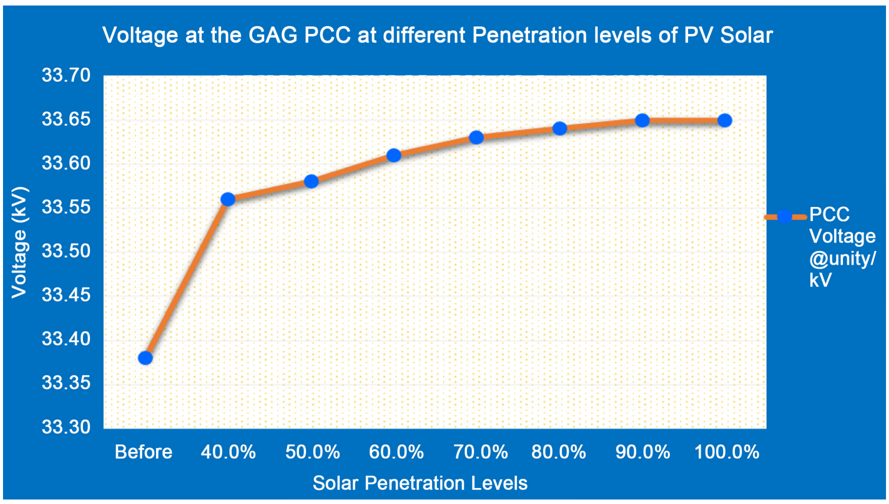

Figure 13. Voltage profile at the GAG PCC (Midway) at different penetration levels of solar PV.

The network losses followed the usual U-Shape trajectory, as the PV capacities interconnected at the GAG PCC increases, with the minimum losses occurring at 40% penetration that corresponds to a capacity of 9 MWp as shown in Figure 14.

5.3. PV Connected at the Darmang Primary Substation—Tail End of Network

The Solar PV was connected at the tail end of the 33 kV-network at the Darmang

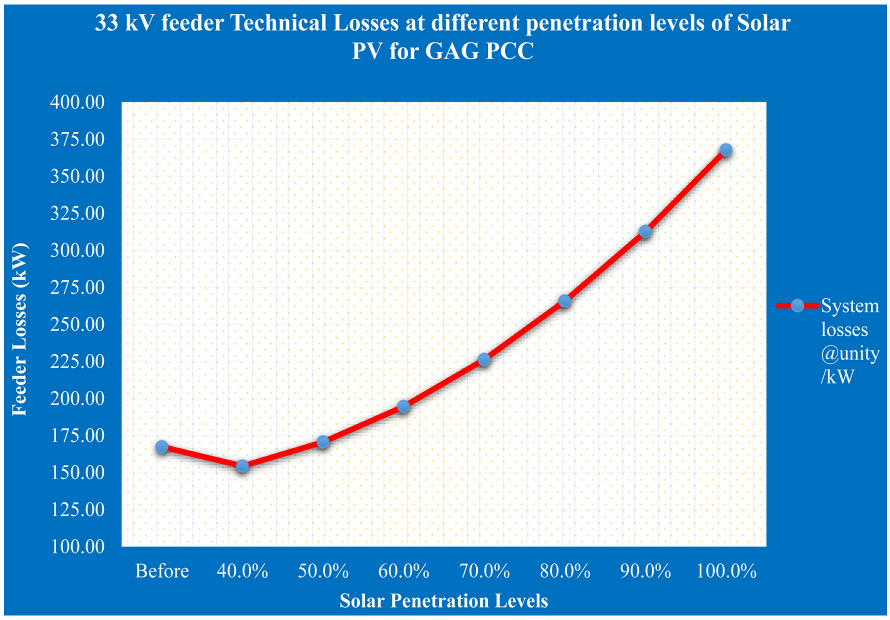

Figure 14. 33 kV technical losses of the Atuabo BSP network at different penetration levels of solar PV for GAG substation (Midway).

Switching substation. The detailed results of the study have been presented in Table 6. The voltage profiles at the Darmang PCC (tailend) and technical losses of the 33 kV at different Solar PV penetration levels are shown in Figure 15 and Figure 16, respectively.

Discussion of Results—Connection of Solar PV Plant at Darmang Primary Substation (Tail End)

As the PV penetration levels increase, the voltage profile improves, but nevertheless remains below ECG's allowable voltage upper limit of 35.97 kV, as shown in Figure 15. The general improvement in the voltage profile with increasing PV penetration as evidenced in Figure 15, adds to the known and published facts in many journals that distributed PV injections in a power system is a useful tool for voltage regulation.

Besides, the network losses followed the usual a U-Shape trajectory, as the solar PV capacities at the Darmang PCC (tail end) were increased, with the minimum losses occurring at 40% penetration that corresponds to a capacity of 9 MWp, as shown in Figure 16.

It is noteworthy, that the U-shape trajectory nature of the network losses with increasing solar PV penetration levels at the PCC, is a feature that is well corroborated in other published works.

5.4. Determination of Optimum Location and Capacity of Solar PV Plant

1) The average bus voltages recorded at Tarkwa (Old Atuabo), GAG and Darmang for the different penetration levels were 33.65 kV, 33.61 kV and 34.00 kV, respectively.

Table 6. Detailed results with Darmang primary substation as the PCC (tail end).

	Interconnected at Damang-Bus							
Network load capacity	22.70	MW	250	Wp				
Total load in kW	22,704.81							
Power Factor of load	0.90							
Penetration level	Before	40.0%	50.0%	60.0%	70.0%	80.0%	90.0%	100.0%
		9.08	**11.35**	**13.62**	**15.89**	**18.16**	**20.43**	**22.70**
Solar PV		9.08	11.35	13.62	15.89	18.16	20.43	22.70
No. of series		16	16	16	16	16	16	16
No. of parallel		2275	2843	3412	3980	4550	5120	5690
100% output (kW)		9081.93	11,352.41	13,622.89	15,893.37	18,163.85	20,434.33	22,704.81
Qty of panels		9,101,926	11,372,407	13,648,000	15,920,000	18,200,000	20,480,000	22,760,000
BSP Voltage@unity/kV	33.70	33.67	33.66	33.65	33.64	33.62	33.60	33.58
PCC Voltage@unity/kV	32.70	33.63	33.81	33.97	34.11	34.24	34.35	34.42
BSP pf@unity/%	89.66	58.44	38.07	12.99	−11.70	−31.55	−45.68	−55.09
PCC pf@unity/%	90.31	−99.92	−99.87	−99.82	−99.76	−99.69	−99.62	−99.52
System losses@unity/kW	167.320	155.880	240.480	357.480	506.960	688.360	901.500	1149.850

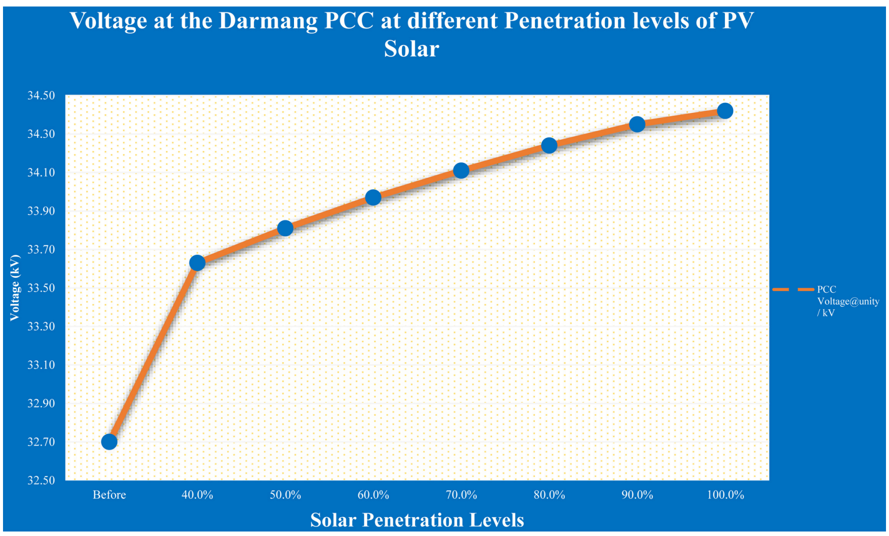

Figure 15. Voltage profile at the Darmang PCC (tail end) at different penetration levels of solar PV.

2) Since all these voltages fall within the acceptable ECG voltage range of between 30.03 kV and 35.97 kV, voltage was not used as a criterion for determining the optimum location and capacity of the Solar PV plant to be connected to the Atuabo BSP network.

3) The reduction in system losses was therefore the sole criterion considered for the determination of the optimum location and capacity of the Solar PV plant to be connected to the Tarkwa (Old Atuabo) BSP network. Figure 17

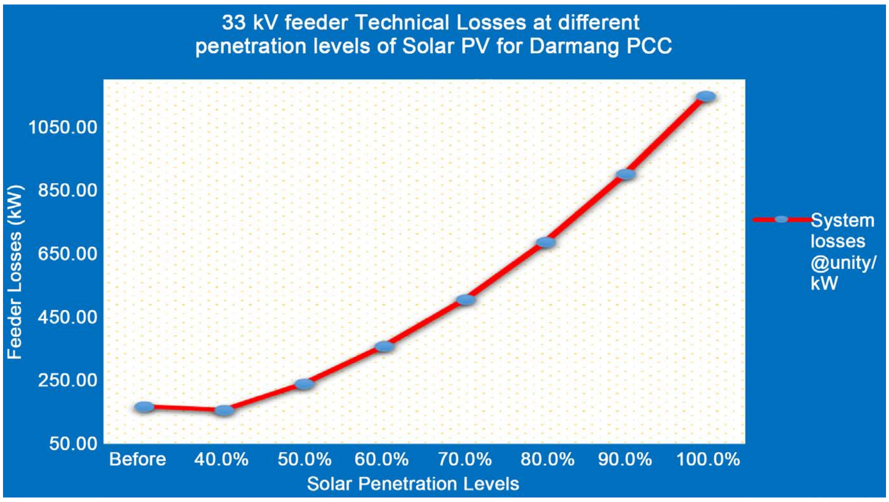

Figure 16. 33 kV feeder technical losses of the Atuabo BSP network at different penetration levels of solar PV for Darmang PCC (tail end).

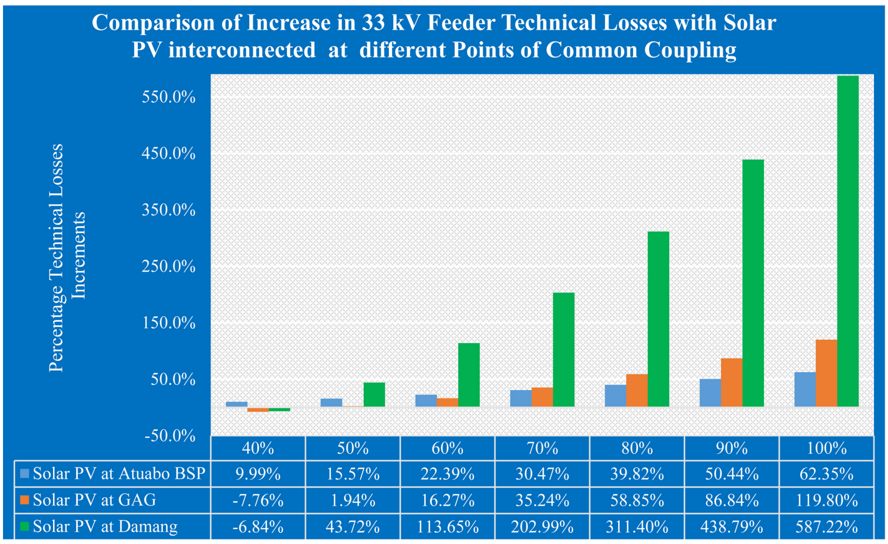

Figure 17. Comparison of reduction in 33 kV system losses with solar PV interconnected at different PCC.

shows the comparison of reduction in 33 kV system losses with the Solar PV interconnected at Old Atuabo (Source), GAG (Midway) and Darmang (tail end) and at the different penetration levels.

4) From **Figure 17**, it is seen that significant loss reductions were obtained at the optimum penetration level of 40% (9 MW). At that penetration level, connecting the Solar PV plant at the GAG PCC (midway) and Darmang PCC (tail end) gave loss reductions (minus sign) of 7.76% and 6.84%, respectively. However, PV integration at the Atuabo BSP (source) rather gave an increment (positive sign) of 9.99%.

5) Beyond the optimum 40% value, it is generally seen that comparatively, the rate of increase in system losses is high.

6) Comparing the GAG and Darmang PCCs, it is noted that, the rate of in-

crease in the system loss with increasing penetration level is far slower for the interconnection at GAG PCC (midway) as compared to Damang PCC (tail end).

7) From the above analysis, the optimum capacity of Solar PV plant to be connected to the Tarkwa (Old Atuabo) BSP network is 9 MWp and the optimum location is the Ghana Australia Gold (GAG) Primary Substation.

5.5. Determination of Optimum Power Factor of Solar PV Inverter

Power flow simulation was conducted for the optimum Solar PV capacity of 9 MWp connected to the GAG Primary Substation at varying power factors (0.85 - 1.0).

Figure 18 shows the percentage loss as a function of the power factor of the solar PV inverter.

From **Figure 18**, the optimum power factor of the 9 MWp Solar PV plant inverter to be interconnected at the GAG Switching Station is seen as 0.94. This is because, below and beyond this power factor, the losses in the network begin to increase.

5.6. Stiffness Ratio of the Point of Common Coupling

The stiffness ratio (SR) at the Point of Common Coupling was determined to assess the impact of the connection of the optimum value of 9 MWp Solar PV plant at the optimum location of GAG PCC.

From **Table 7**, the stiffness ratio of the anticipated three phase fault capacity to the Solar PV Plant capacity is 41.9 which is far greater than the standard industrial minimum value of 5.

With reference to the international best practice, this higher value of 41.9 is an indication that there will not be any voltage control problems in the operation of the proposed Solar PV interconnection.

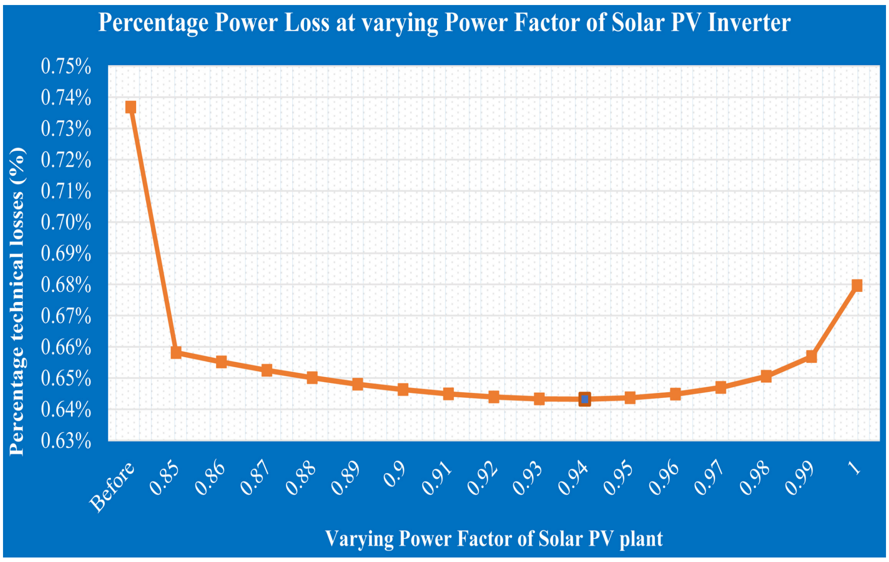

Figure 18. Percentage power loss at varying power factor of solar PV inverter.

Table 7. Stiffness ratio of three phase fault level at optimum PCC to the optimum plant capacity.

Bus Name	3-Phase Fault ($MVA_{3Ø\text{-}sc}$)	Capacity supplied by DG PV(MVA_{sp})	Stiffness Ratio (MVA3Ø-sc)/(MVAsp)	Remarks
PCC at GAG 33 kV bus	404.4	9.7	41.9	The ratio of the available short circuit capability at PCC to the PV plant size gave a value greater than 5

6. Conclusions and Recommendations

6.1. Conclusions

In this research work, simulation studies have been conducted using the CYME software (Cyme 8.0 Rev 05) to determine the optimum penetration level and location for solar PV integration into the Tarkwa (Old Atuabo) 33 kV BSP network in the Western Region of Ghana, and operated by the Electricity Company of Ghana (ECG). Besides, the stiffness ratio of the optimum location, as well as the optimum power factor of the solar PV inverter, has been determined.

Using losses reduction as the criterion, the optimum penetration level was determined as 40%, corresponding to 9 MWp solar PV plant output. For the three main PCCs, the Ghana Australia Gold (GAG) Substation was determined to be the optimum location for integration, yielding the highest system loss reduction. This GAG substation happens to be the midway PCC in the case study network.

Also, the stiffness ratio at the GAG Substation was determined as 41.9, a value far higher than the industrial standard minimum value of 5. This high value of SR indicates that the integration of the Solar PV Plant at the GAG Switching Station will create very few voltage regulation problems. In addition, the optimum power factor of the PV plant was determined to be 0.94 lagging.

Furthermore, increasing solar PV penetration levels generally resulted in improvement in the voltage profiles of the 33 kV network; the improvements were all nevertheless within the ECG's allowable voltage range of between 30.03 kV and 35.97 kV. This upper value represents a 1.97% increase in the voltage profile of the 33 kV network.

A maximum of 7.76% system loss reduction was attained. Also, the network losses followed the usual U-shape trajectory with increasing solar PV penetration levels at the PCC, a feature that is corroborated in other published works.

6.2. Recommendation

It is recommended that stability studies be carried out on the Tarkwa (Atuabo) BSP network to further analyze the stability condition of the Tarkwa BSP with the integration of solar PV to it.

Acknowledgements

The authors wish to thank the Electricity Company of Ghana (ECG) and The Brew Hammond Energy Centre (TBHEC) of the Kwame Nkrumah University of Science and Technology (KNUST).

Conflicts of Interest

The authors declare no conflicts of interest regarding the publication of this paper.

References

[1] Le Quéré, C. (1997) Greenhouse-Gas Emission Targets for Limiting Global Warming to 2˚C. *Agricultural and Forest Meteorology*.

[2] Zahedi, A. (2011) Maximizing Solar PV Energy Penetration Using Energy Storage technology. *Renewable and Sustainable Energy Reviews*, **15**, 866-870. https://doi.org/10.1016/j.rser.2010.09.011

[3] Chalmers, S.M., Hitt, M.M., Underhill, J.T., Anderson, P.M., Vogt, P.L. and Ingersoll, R. (1985) The Effect of Photovoltaic Power Generation on Utility Operation. *IEEE Transactions on Power Apparatus and Systems*, **PAS-104**, 524-530. https://doi.org/10.1109/TPAS.1985.318968

[4] Povlsen, A.F. and A/S, E. (2002) Impacts of Power Penetration from Photovoltaic Power Systems in Distribution Networks. *International Energy Agency-Implementing Agreement on Photovoltaic Power Systems*, 1 p.

[5] Farhoodnea, M., Mohamed, A., Shareef, H. and Zayandehroodi, H. (2012) Power Quality Impact of Grid-Connected Photovoltaic Generation System in Distribution Networks. 2012 *IEEE Student Conference on Research and Development*, Pulau Pinang, Malaysia, 5-6 December 2012, 1-6. https://doi.org/10.1109/SCOReD.2012.6518600

[6] Kwofie, E.A., Mensah, G. and Antwi, V.S. (2019) Post Commission Grid Impact Assessment of a 20 MWp Solar PV Grid Connected System on the ECG 33 kV Network in Winneba. 2019 *IEEE PES/IAS PowerAfrica*, Abuja, Nigeria, 20-23 August 2019, 521-526. https://ieeexplore.ieee.org/document/8928841 https://doi.org/10.1109/PowerAfrica.2019.8928841

[7] Gabr, W.I. and Salem, W.A. (2018) Impact of Grid Connected Photovoltaic System on Total Harmonics Distortion (THD) of Low Voltage Distribution Network: A Case Study. 2018 *Twentieth International Middle East Power Systems Conference*, Cairo, Egypt, 18-20 December 2018, 608-614. https://doi.org/10.1109/MEPCON.2018.8635216

[8] Farhoodnea, M., Mohamed, A., Shareef, H. and Zayandehroodi, H. (2013) Power Quality Impact of Renewable Energy based Generators and Electric Vehicles on Distribution Systems. *Procedia Technology*, **11**, 11-17. https://doi.org/10.1016/j.protcy.2013.12.156

[9] Zambri, M.K.M., Aras, M.S.M., Khamis, A. and Hairi, M.H. (2016) Investigating the Impact of Photovoltaic Connection to the Malaysian Distribution System. *Journal of Telecommunication*, *Electronic and Computer Engineering*, **8**, 23-28.

[10] Karimi, M., Mokhlis, H., Naidu, K., Uddin, S. and Bakar, A.H.A. (2016) Photovoltaic Penetration Issues and Impacts in Distribution Network—A Review. *Renewable and Sustainable Energy Reviews*, **53**, 594-605.

https://doi.org/10.1016/j.rser.2015.08.042

[11] Farhoodnea, M., Mohamed, A., Shareef, H. and Zayandehroodi, H. (2012) An Enhanced Method for Contribution Assessment of Utility and Customer Harmonic Distortions in Radial and Weakly Meshed Distribution Systems. *International Journal of Electrical Power & Energy Systems*, **43**, 222-229. https://doi.org/10.1016/j.ijepes.2012.05.013

[12] Shah, H.A. and Ahmad, A.U. (2019) Solar Energy and Duck Curve. **8**, 373-379.

[13] Davoudi, M., Cecchi, V. and Aguero, J.R. (2015) Effects of Stiffness Factor on Bus Voltage Variations in the Presence of Intermittent Distributed Generation. 2015 *North American Power Symposium*, Charlotte, NC, USA, 4-6 October 2015, 1-6. https://doi.org/10.1109/NAPS.2015.7335187

[14] Peng, W., Baghzouz, Y. and Haddad, S. (2013) Local Load Power Factor Correction by Grid-Interactive PV inverters. 2013 *IEEE Grenoble Conference*, Grenoble, France, 16-20 June 2013, 1-6. https://doi.org/10.1109/PTC.2013.6652412

[15] Ghana Districts: Tarkwa-Nsueam Municipal Assembly. http://tnma.gov.gh/about-us/#:~:text=The%20population%20of%20Tarkwa%2DNsuaem,2016%20and%20175%2C868%20in%202017.